

SYNTHESIS AND ANTIBACTERIAL ACTIVITY OF COBALT-THIOUREA NANOPARTICLES ON SELECTED WATERBORNE BACTERIAL PATHOGENS

G. P. MOUKANGOE^a, N. LALOO^a, V. PAKADE^b, F. MTUNZI^b,
M. E. MONAPATHI^b, J. S. MODISE^b, M. J. KLINK^{a,b,*}

^a*Department of Biotechnology, Vaal University of Technology, Andries Potgieter Boulevard, Vanderbijlpark, 1911, South Africa*

^b*Department of Chemistry, Vaal University of Technology, Andries Potgieter Boulevard, Vanderbijlpark, 1911, South Africa*

Traditional water treatment technologies have been used to treat wastewater to ensure continuous supply of pure drinking water. However, these have proved costly and ineffective. The use of nanoparticles, mainly to remove microbial contaminants is becoming a major area of research. The aim of this study was to synthesize, characterize and investigate antimicrobial activity of Cobalt-thiourea nanoparticles against selected waterborne pathogenic bacteria. Cobalt-thiourea nanoparticles with different ratios were synthesized *via* wet chemistry method and characterized through UV-Visible spectroscopy (UV-Vis), photoluminescence spectroscopy (PL), fourier transform infrared spectroscopy (FTIR), transmission electron microscopy (TEM), X-ray diffraction (XRD) and thermogravimetric analysis (TGA). FTIR spectral studies confirmed that the binding of thiourea with cobalt occurs through sulphur. The TGA curves indicated a two-step decomposition for Co-thiourea nanoparticles ratios. Morphology for ratios (1:1, 1:2, 1:3) were around 10-30 nanometers (nm) and dispersed. Ratio 2:1 particles were around 50 nm and agglomerated with irregular shapes. The X-Ray diffraction confirmed amorphous identity for metallic nanoparticles material. Co/thiourea nanoparticles showed strong antimicrobial activity by causing inhibition of growth for a wide range of Gram negative bacteria with low Minimum Inhibitory Concentration (MIC) values. Further research on metallic nanomaterials in water purification systems is needed to overcome the spread of waterborne bacterial infections and antimicrobial resistance.

(Received May 20, 2020; Accepted August 7, 2020)

Keywords: Pathogenic bacteria, Cobalt nanoparticles, Antimicrobial activity

1. Introduction

Deteriorating water quality has rendered safe drinking water a challenge in developing and developed countries [1]. Sustainable Development Goal (SDG) 3 set in 2015 by the United Nations General Assembly agreed on good health and well-being for people and our planet by 2030. The directives are to combat waterborne diseases and reduce death and illness from unsafe water, unsafe sanitation, and lack of hygiene. Furthermore, SDG 6 decided on the provision of access to clean water and sanitation for people and our planet by 2030. The plan of action was set on the management and sustainability of water resources [2]. Surface water resources are a source of potable water after treatment and domestic water without treatment. Due to lack of or improper wastewater treatment facilities, wastewater and its effluents are often released into surface water sources [3]. The waste water discharges elevate freshwater pollution and deplete clean water resources [4].

Increased microbial pathogens and poor water quality resulting from waste water effluents pose serious health hazards to people situated downstream from or near municipal sewage outfalls or contaminated water [5]. Waterborne related infections/diseases continue to be a major public health threats in many countries [6]. Continuous exposure and misuse of antimicrobial agents has

* Corresponding author: michaelk1@vut.ac.za

resulted in the development of drug resistance from pathogenic microbes. The prevention and treatment of an ever-increasing range of infections is threatened [7].

Wastewater effluents should be treated properly for pathogenic microbes to prevent the spread of infection/diseases [3]. The traditional water treatment processes that include adsorption, precipitation, ion exchange, reverse osmosis, electrochemical treatments, membrane filtration, evaporation, floatation, oxidation, and biosorption have proved costly and ineffective in removing the wide spectrum of toxic chemicals and pathogenic microorganisms in raw water [8, 9].

Nanotechnology has received great attention in treating persistent and emerging contaminants [1]. According to Ayanda and Petrik (2014), it offers low cost, reusable and highly efficient ways of removing and recovering microbial and wastewater pollutants [10]. The surface-to-volume property of metal and metal-oxide based nanoparticles enable them to differentiate bacterial cells from mammalian cells. This provides long-term antibacterial activity and biofilm prevention [11]. Moreover, application of metal containing nanoparticles have improved waste treatment methods by inducing coating on pollutants to restrain toxicity of compounds and killing of pathogens in waste water environment. The magnetic property of metal nanomaterials enables their recovery by a magnet after adsorption. This facilitates their use in the field of catalysis and wastewater treatment applications [12].

Metal- and metal-oxide-based nanoparticles: Silver, iron, zinc, titanium dioxide, zinc oxide and iron oxide have been used to treat microbial pollutants in wastewater [13, 14]. Outbreaks from waterborne infections are on the rise and there is a need for further research on the use of nanotechnology approach to purifying water for safe human consumption. The aim of the present study was to synthesize, characterize and investigate antimicrobial activity of Cobalt-thiourea (Co/thiourea) nanoparticles on selected waterborne pathogenic bacterial species.

2. Experimental details

2.1. Materials details/chemical details

All the chemicals used for synthesis were used without any further purification. Titanium tetrabutoxide, acetic acid, ethanol, sodium borohydride, silver nitrate and PVP were purchased from Sigma Aldrich, South Africa.

2.2. Synthesis of Cobalt-thiourea nanoparticles

$\text{CoCl}_2 \cdot 6\text{H}_2\text{O}$ (4.76 g) was dissolved in 30 mL n-butanol. Subsequently, 6.08 g of thiourea was added. The mixture was heated and refluxed for three hours on heating to completely dissolve the entire solid state. The solution was cooled to room temperature. Thereafter, benzene was added until a slightly permanent turbidity formed. The complex was cooled in an ice chest. Afterwards, a blue solid precipitate formed. The precipitate was filtered and washed twice with ethanol and acetone under vacuum [15].

2.3. Characterization

The prepared Cobalt-thiourea nanoparticles were characterized for their optical and structural properties.

2.3.1. UV-Visible spectroscopy (UV-Vis)

The sample was prepared by dissolving the nanoparticles with distilled water to make a dilute sample solution and sonicated for 60 minutes. The UV-Vis was turned on to warm the lamps. A cuvette was filled with the distilled water and placed inside the spectrophotometer to read the blank results for the absorbance spectrum. This serves as blank control and helps account for light losses due to scattering or absorption by the solvent. The cuvette was rinsed twice with the diluted nanoparticles. The cuvette was filled quarter full and placed in the spectrophotometer in the correct direction and covered to prevent any ambient light. Absorbance spectrum was collected by allowing the instrument to scan through different wavelengths to collect the absorbance [16].

2.3.2. Photoluminescence spectroscopy (PL)

The sample was prepared by dissolving the nanoparticles with distilled water to make a dilute sample solution and sonicated for 60 minutes. The UV-Vis was turned on to allow the lamps to warm up. A cuvette was filled with the distilled water and placed inside the spectrophotometer to read the blank results for the absorbance spectrum. This serves as blank control and helps account for light losses due to scattering or absorption by the solvent. The cuvette was rinsed twice with the diluted nanoparticles. The cuvette was filled quarter full (the cuvette should be clean of any fingerprints) and placed in the spectrophotometer in the correct direction and covered to prevent any ambient light. Absorbance spectrum was collected by allowing the instrument to scan through different wavelengths to collect the absorbance [16].

2.3.3. Fourier transform infrared spectroscopy (FT-IR)

Fourier transform infrared spectroscopy absorption spectrum of nanoparticles was obtained from 16 scans at a resolution of 4 cm^{-1} in the region of $400\text{--}4000\text{ cm}^{-1}$ using a Bomem MB-120 FT-IR spectrometer that is equipped with a potassium bromide beam splitter and a deuterated triglycine sulphate (DTGS) detector. To prepare the samples, a small quantity of freeze-dried nanoparticles was deposited on potassium bromide tablet surface prior to FT-IR analysis [17].

2.3.4. Transmission electron microscopy (TEM)

Transmission electron microscopy images were recorded by JEOL JEM 1010 transmission electron microscope equipped with an AMT XR40 digital imaging camera at a magnification of 1000 x and a maximum accelerating voltage of 10 kV. Samples were dispersed in ethanol and it was ultra-sonicated for 20 minutes. A drop of nanoparticles suspension was coated onto the copper grid, followed by negative staining with an aqueous solution of uranyl acetate at 1% (w/v). Particles diameter of approximately 300 randomly selected nanoparticles from different TEM micrographs was determined using the morphometry software image JV, 1.44 [18].

2.3.5. X-ray diffraction (XRD)

The phase identification of the crystalline nanoparticles was carried out by XRD on a D8 diffractometer using secondary graphite mono-chromated $\text{Cu K}\alpha$ radiation ($\lambda = 1.54060\text{ \AA}$) at 40 kV/50mA. Measurements were taken using a glancing angle of incidence detector at an angle of 2° , for 2θ values over $20^\circ\text{--}60^\circ$ in steps of 0.05° with a scan speed of $0.01^\circ 2\theta \cdot \text{s}^{-1}$.

2.3.6. Thermogravimetric analysis (TGA)

The sample preparation for thermogravimetric analysis was done by weighing 10 mg of the complexes. These complexes were decomposed at temperature range of $50\text{--}930^\circ\text{C}$. This analysis was performed on a Perkin Elmer Pyris 6 TGA under an inert atmosphere of dry nitrogen, and heating rate of $10^\circ\text{C} \cdot \text{min}^{-1}$.

2.4. Antimicrobial susceptibility tests

The antibacterial activity of synthesized nanoparticles was tested against the following gram-negative bacterial species: *Escherichia coli* ATCC O157, *Pseudomonas aeruginosa* ATCC 10145, *Shigella sonnei* ATCC 25931, *Salmonella enterica* ATCC 35664, and *Salmonella typhi* ATCC 33458. The test organisms were grown in nutrient broth on a shaker incubator at 150 rpm for 24 hours at 37°C to attain the colony-forming unit (CFU) of $\sim 10^6$ per/ml.

2.4.1. Agar well diffusion method

Preliminary antimicrobial susceptibility testing was assessed by agar well diffusion method [19]. One-hundred microliters of each overnight bacteria culture was spread on Mueller-Hinton (MH) (Biolab Merck, Germany) agar plates. A hole with a diameter (6 to 8 mm) was punched on the agar plate aseptically with sterilized micropipette tips and $20\text{ }\mu\text{L}$ of doped Cobalt nanoparticles ratios (1:1, 1:2, 1:3, 2:1 $\mu\text{g}\cdot\text{mL}^{-1}$) were introduced into the wells. Commercial standard antibiotic, neomycin ($20\text{ }\mu\text{m}$) was used as a positive control. The sensitivities of the test

organisms to the different Cobalt-thiourea nanoparticles and neomycin were indicated by clear zone (in mm) (zone of inhibition) around wells after 24 hours of incubation at 37°C.

2.4.2. Minimum Inhibitory Concentration

Minimum inhibitory concentration (MIC) investigations were conducted to determine whether various Cobalt-thiourea nanoparticles concentrations have inhibitory effect on the growth of bacteria. Bacterial species were incubated for 24 hours at 37°C in Mueller Hinton broth (MHB) (Biolab Merck, Germany) at different ratios (1:1, 1:2, 1:3, 2:1 $\mu\text{g.mL}^{-1}$) of doped Cobalt-thiourea nanoparticles. MIC were determined by serial two-fold dilutions from concentrations (156-1.22 $\mu\text{g.mL}^{-1}$). Ten microliters of the overnight-grown culture were inoculated into 96-well micro-plate with 0.02% resazurin dye. A two-fold dilution of neomycin (20 mg.mL^{-1}) was used as a positive control. The control group did not contain Cobalt-thiourea nanoparticles. The plates were incubated aerobically at 37°C and subsequently inspected for colour change.

2.5. Statistical analysis

Statistical data were analysed using Microsoft Excel (2016) to determine averages and standard deviations. Statistically significant differences between diameter of inhibition zones were determined by student t-test. Significance level was set at $p = 0.0001$.

3. Results and discussion

3.1. Optical properties

UV-Vis spectroscopy was used to investigate the optical properties of Cobalt-thiourea at various ratios 1:1, 1:2, 1:3 and 2:1. Absorbance bands were observed at 290 nm and 590 nm with a tail extending towards the longer wavelengths as a result of quantum size effects (Fig. 1).

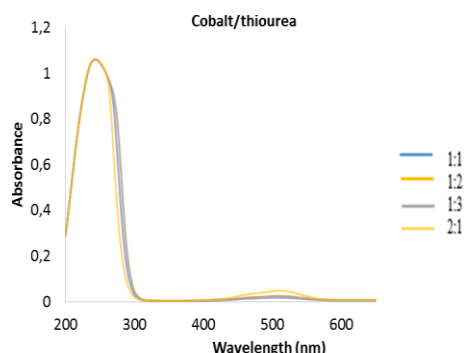


Fig. 1. UV – Vis absorption spectrum of Cobalt/thiourea nanoparticles.

The absorption band gaps are blue shifted to a high energy compare to bulk cobalt with respect to reduced particle size of the material. The blue-shift in band-edge was further explained using the work reported by Yao et al. (2003) [20]. They discovered that not only the size of the nanoparticles has an influence on the band-gap but shape also plays an important role. Therefore, the blue-shifts in band-edge can be explained by the notion that the morphology (length and width of rods) of the particles has a great influence on the optical properties of the nanoparticles. With spherical particles, the diameter of the particle can be related to the optical properties of the particles, whereas with rod or wire-like particles, the diameter does not account for the properties of the particles. Other reason accounting for the blue shift can be associated with the agglomeration of the particles due to ageing and external factors such as oxygen to penetrate into the pores of the particles [21].

Transition state in CoS exists in several numbers, according to Gupta and co-workers the two maxima in absorbance are because of bulk state transition and surface transitions. The surface

states include the localized states because of defect in bulk in addition to the surface states. The optical transition to and from the surface states will produce maxima at higher wavelengths [22].

Photoluminescence (PL) activity was determined using fluorescence spectrometer in order to evaluate how well the photo-generated electrons and holes are effectively separated by these nanoparticles. Red shift from the respective band edges of the absorption spectra. The excitonic emission usually gives sharp peaks near their band edges. The narrowing of the peaks is observed as the monomer concentration is increased due to excitonic type of emission. Emission peak has a narrow shape, around 510 nm, which indicates the mono-dispersity and good passivation of the particles (Fig. 2). Photoluminescence emission maxima of the samples were observed and are red shifted from their respective band edges of the absorption spectra [21].

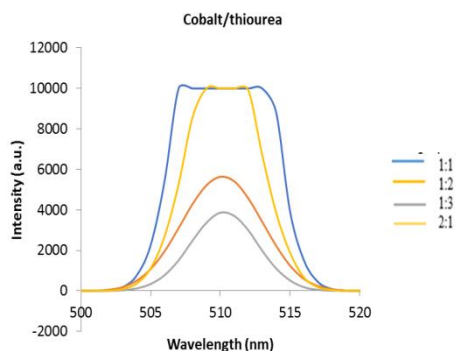


Fig. 2. PL graph of Cobalt-thiourea complex.

3.2. Functional groups and morphological analysis

In order to determine the surface functional groups of the Cobalt-thiourea ratios, the FTIR spectra analysis was carried out and the spectra are presented in Fig. 3. The spectrum showed a decrease in the frequency shifts to 1484 and 1487 cm^{-1} , respectively on coordination of the sulphur atom to the Co-metal. The N-H absorption bands are not shifted to the lower frequency which indicates that the nitrogen expected to bond Co is not present and the bonding must be between the sulphur and the Co-metal. These absorption bands include: N-H stretching symmetric at 3189 cm^{-1} ; N-H stretching asymmetric at 3390 cm^{-1} ; and N-H rocking at 1099 cm^{-1} . Similarly, from the N-C-N stretching mode at 1472 cm^{-1} there are no observable features of the Co-N bond but much enhanced sensitivity to coordination through sulphur. The free ligand shows a band observed at 732 cm^{-1} , which is due to contribution of C-S stretching and has shifted to a lower frequency 721 cm^{-1} Co/thiourea. This signifies a decrease in the double bond character of the C=S which confirms the sulphur bonding of thiourea to cobalt [23]. The formation of hydrogen bond expected to increase the contribution to highly polar character for nitrogen to carbon and sulphur to carbon. The bands observed at 2000 to 2700 cm^{-1} also confirms the formation of the Co/thiourea compound, because delocalization of pi electrons of thiourea occur at these regions [24, 25, 26].

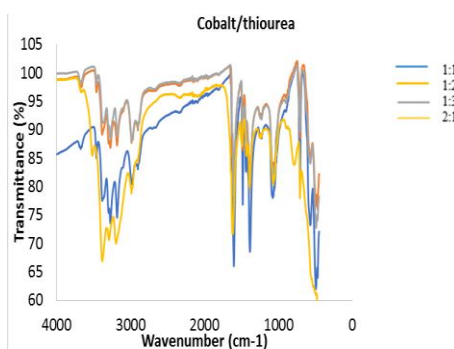


Fig.3. FTIR spectra of Cobalt/thiourea complex.

The Transmission Electron Microscope was employed to investigate the size and the morphology of the Cobalt-thiourea nanoparticles. TEM micrographs showed particles from ratios 1:1, 1:2 and 1:3 well dispersed (Fig. 4) due to their small size and high surface energy. The particles appear to be around 10 to 30 nanometers in size. At ratio 2:1, particles are agglomerates with irregular shapes of about 50 nm [27].

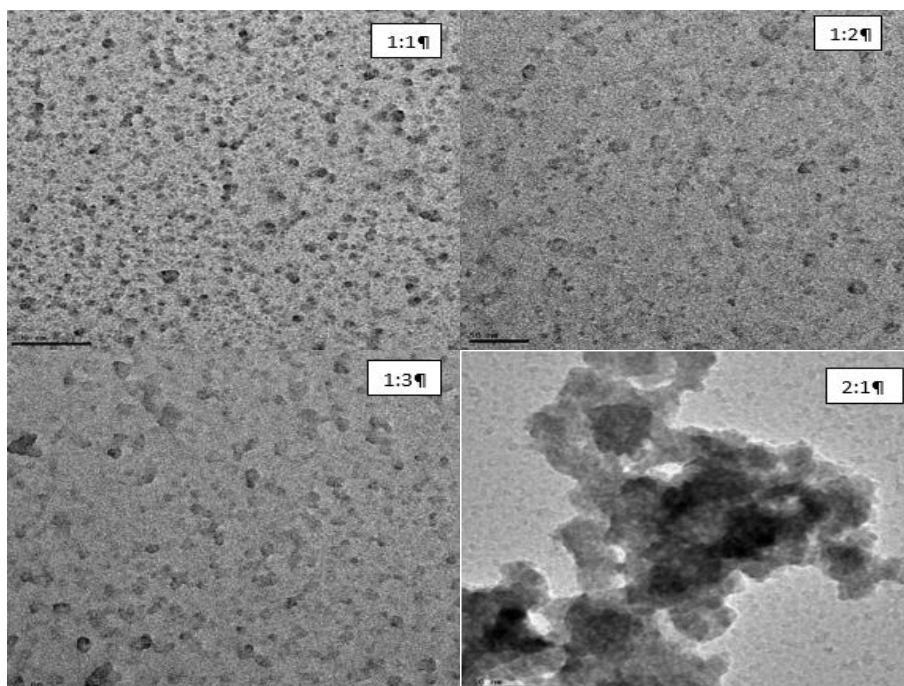


Fig. 4. TEM image for Cobalt/thiourea nanoparticles.

3.3 Structural properties and thermogravimetric analysis

The powder X-Ray diffraction (Fig. 5) was used to obtain details of the phase and crystallite sites of the Cobalt-thiourea nanoparticles ratios. The diffraction peaks show a lot of impurities which might be as a result of insufficient washing of nanoparticles or recurring of impurities from the complex. The Bragg peaks are not well defined, which means the material is amorphous [28].

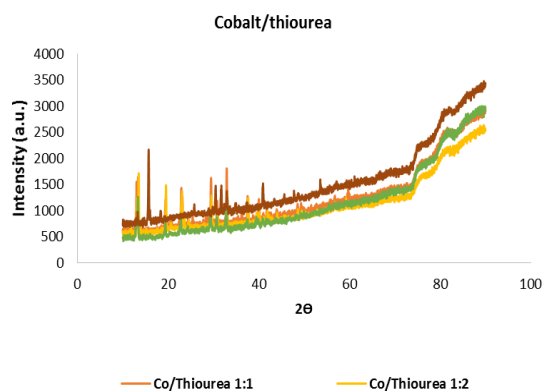


Fig. 5. XRD patterns of Cobalt-thiourea complexes.

Thermogravimetric analyses was used determine Cobalt-thiourea ratios thermal stability and its fraction of volatile components by monitoring the weight change that occurs as a sample is heated at a constant rate. The TGA curves (Fig. 6) indicate the two-step decomposition for Co/thiourea complexes (1:1, 1:2, 1:3). Ratio 1:2 (not shown) reacted similar to other metallic particles ratios because they are burned at constant temperatures. The ratios on Co/thiourea complexes display first decomposition at 200°C to 300°C. This accounts for 80 to 82% mass loss observed across all ratios. According to Thendral et al. (2018), thiourea are lost at 180 to 300°C [27]. There is a slow weight loss (20%) of the ratios complexes which led to the formation of metal sulphide and oxide at a final temperature of 800°C [20]. The high thermal stability of Co/thiourea arises due to strong bond existing between the conjugation layers of thiourea urea molecule and the metal ions. The thermogravimetric study thus confirm the formation of the title compound in the stoichiometric ratio and the decomposition pattern of [29].

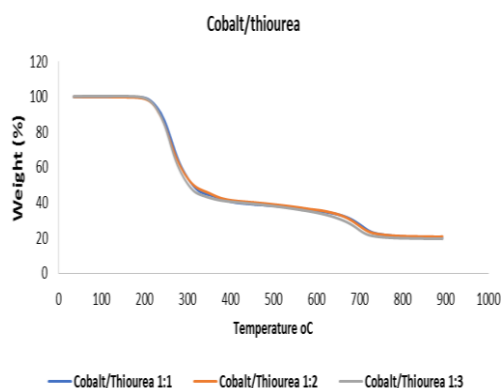


Fig. 6. TGA curves for Co/thiourea complexes.

3.4 Screening of antimicrobial activity

The antimicrobial activity of Co-thiourea nanoparticles was investigated against bacterial species using the agar well diffusion assay. Variable antibacterial activities against bacterial growth were observed. The zones of inhibition (mm) are recorded in **Table 1**. Pathogenic bacterial isolates were more sensitive (larger zone of inhibition) to neomycin than Co/thiourea nanoparticles. The zone of inhibitions of cobalt metal complex were *Salmonella typhi* ATCC 33458 (3.32 mm), *Shigella sonnei* ATCC 25931 (3.15 mm), *Escherichia coli* ATCC O157 (2.4 mm), *Pseudomonas aeruginosa* ATCC 10145 (2.3 mm) and *Salmonella enterica* ATCC 35664 (1.54 mm). Highest antimicrobial activity was observed against *Salmonella typhi* ATCC 33458. A study by Moradpoor et al. (2019) conformed to the present study; high antimicrobial activity was observed on a commercial drug, gentamycin than Cobalt nanoparticles [30]. However, in a study by Jeevignunta and Navva. (2017), metallic nanoparticles were more effective than ampicillin and streptomycin [31].

Table 1. Minimum Inhibitory Concentrations and diameters of zone of inhibition (averages and standard deviations) of bacterial species.

Bacterial pathogens	Minimum Inhibitory Concentrations (MIC)					Agar well diffusion method			
	Co/thiourea nanoparticles (mm)				Neomycin (mm)	Co/thiourea nanoparticles (mm)	Neomycin (mm)	Student t-test	
	1:1	1:2	1:3	2:1					
<i>Escherichia coli</i> ATCC O157	78.25	78.35	39.06	0.0	4.88	2.4±1.86	9.6±1.68	p = 0.0001	
<i>Pseudomonas aeruginosa</i> ATCC 10145	78.25	39.06	39.06	19.55	9.76	2.3±1.86	6.8± 0.13	p = 0.0001	
<i>Shigella sonnei</i> ATCC 25931	156.2 5	78.25	39.06	39.06	9.76	3.15±0.88	10.43±0.54	P= 0.0001	
<i>Salmonella enterica</i> ATCC 35664	156.2 5	156.2 5	156.25	156.2 5	4.88	1.54±1.25	13. 35±2.81	p = 0.0001	
<i>Salmonella typhi</i> ATCC 33458	156.2 5	78.25	39.09	19.55	4.88	3.32±1.92	14.26±0.0	p= 0.0001	

Minimum inhibitory concentrations in the present study indicated that the bacterial isolates were inhibited from growth by the varying concentrations of Co-thiourea nanoparticles. Resazurin dye designates cell viability by changing from a blue/ non-fluorescent state to a pink/ highly fluorescent state. The colour change results from chemical reduction from aerobic respiration due to cell growth [32]. The concentration at which no change in colour was noted was taken as MIC. MIC for neomycin and Co-thiourea nanoparticles ratios were 4.88 and 19.55. MIC results show neomycin as the better antimicrobial agent against pathogenic bacterial species and this correlates with the agar well diffusion assay results. The Co-thiourea nanoparticles ratios: 2.1 was more effective than other metallic nano-preparations. However, conflicting results were observed for *E. coli* ATCC O157, which showed no growth inhibition when exposed to Co-thiourea nanoparticles ratio 2.1.

Microorganisms in the present study are pathogens causing waterborne disease outbreaks. They are known to cause mild to severe fatal infectious diseases in human such as diarrhoea, gastroenteritis, salmonellosis, shigellosis, typhoid fever, urinary tract and kidney infections [33, 34, 35]. Their occurrence in WWTPs would not be surprising as these are known to harbour pathogens [36]. Pathogenic species cause morbidity and mortality in human; moreover, their prevention and treatment is costly [33]. Amin et al. (2014) and Samanta et al. (2016) have reported on the classical methods to remove pathogenic microorganisms in raw water and the exercise proved expensive and ineffective [8, 9]. The use of metallic nanoparticles in treating these pathogenic microbes would become an answer in terms of cost and effectiveness [10, 37]. Antimicrobial resistance as a global challenge and the use of nanoparticles would become the next best solution to microbial water treatment, better water quality and improved health.

4. Conclusions

Classical wastewater treatment methods have proved ineffective and costly. The growing antimicrobial resistance from continuous exposure of pathogenic microorganisms with antimicrobial agents is a public health risk. Pathogenic bacterial infections may become lethal due to the development of drug resistance. The uses of metallic nanoparticles in treating wastewater especially pathogenic microbes has gained interest in research. The present study successfully

synthesized, characterized Cobalt-thiourea nanoparticles with different ratios and tested for their antimicrobial activity.

The synthesis of Cobalt-thiourea nanoparticles, especially for antibacterial purposes against human pathogens paves a way in the discovery of antibacterial drugs. The metallic nanoparticles effectively inhibited the growth of pathogenic test microbes at varying zones of inhibition and low MIC. Antimicrobial resistance is a global health challenge. Metallic nanoparticles nanomaterials have a huge potential to treat polluted water. Their applications would become the next best solution to microbial water quality problems and improved public health.

Acknowledgements

The authors would like to thank National Research fund (NRF) for financial support and the Departments of Biotechnology and Chemistry at Vaal University of Technology for providing necessary laboratory facilities to accomplish this work. The views expressed are those of the authors and not of the funding agency.

References

- [1] T. C. Prathna et al., *Separation and Purification Technology* **199**, 260 (2018).
- [2] United Nations Development Program (UNDP), Sustainable Development Goals (SDGs). <https://www.undp.org/content/undp/en/home/sustainable-development-goals.html>. Date of access: 10-04-2020 (2015).
- [3] J. N. Edokpayi et al., Impact of wastewater on surface water quality in developing countries: A case study of South Africa. In *Water Quality, 2017*, INTECH, Vienna, Austria, p. 401 (2017).
- [4] Avalon Global Research, Water and waste water treatment opportunity in India. An Overview. http://www.export.gov.il/uploadfiles/02_2012/indiawater.pdf. Date of Access: 21-April-2020 (2011).
- [5] S. Naidoo, A. O. Olaniran, *International Journal of Environmental Research and Public Health* **11**, 249 (2014).
- [6] World Health Organization (WHO), Water, Sanitation and Hygiene strategy 2018-2025, Geneva. (WHO/CED/PHE/WSH/18.03). Licence: CC BY-NC-SA 3.0 IGO (2018).
- [7] F. Prestinaci et al., *Pathogens and Global Health* **109**, 309 (2015).
- [8] M. T. Amin et al., *Advances in Materials Science and Engineering* **82**, 5910, 24 (2014).
- [9] H. S. Samanta et al., *Austin Chemical Engineering* **3**(3), 1036 (2016).
- [10] O. S. Ayanda, L. F. Petrik, *International Journal of Chemical, Material and Environmental Research* **1**(1), 1 (2014).
- [11] K. Gold et al., *Advances in Therapy*, 1 (2018).
- [12] S. Naz et al., *Advances in Chemistry*, 1 (2014).
- [13] F. Lu, D. Astruc, *Coordination Chemistry Reviews* **356**, 147 (2018).
- [14] S. Singh, V. Kumar, R. Romero, K. Sharma, J. Singh, Applications of nanoparticles in wastewater treatment. In: *Nanobiotechnology in Bioformulations, Nanotechnology in the Life Sciences*, R. Prasad, V. Kumar, M. Kumar, D. Choudhary, Editors. 2019, Springer, Cham, p. 395-418.
- [15] R. Amutha et al., *Journal of Nanoscience and Nanotechnology* **11**, 7940 (2011).
- [16] K. R. Nemade, S. A. Waghuley, *Results in Physics* **3**, 52 (2013).
- [17] K. Zhang et al., *Water Science and Technology* **63**, 2542 (2011).
- [18] R. Saravanan et al., *RSC Adv.* **5**, 34645 (2015)
- [19] S. Magaldi et al., *International Journal of Infectious Diseases* **8**, 39 (2004).
- [20] J. Yao et al., *Journal of Materials Science Letters* **22**, 1491 (2003).
- [21] Y. Wang et al., *Cell Regulation* **2**(6), 453 (1991).
- [22] K. Gupta et al., *Beilstein J Nanotechnol* **4**, 345 (2013).
- [23] M. J. Moloto et al., *Journal of Chemistry* **3**, 1 (2013).

- [24] R. Rajasekaran et al., *Materials Chemistry and Physics* **82**, 273 (2003).
- [25] A. More et al., *Journal of Thermal Analysis and Calorimetry* **94**, 63 (2008).
- [26] G. Madhurambal et al., *Journal of Thermal Analysis Calorimetry* **119**(2), 931 (2015).
- [27] M. Thendral et al., *International Journal for Research in Engineering Application and Management* **04**(06), 319 (2018).
- [28] W. H. Bragg, W. L. Bragg, *Proceedings of the Royal Society of London* **88**, 428 (1997).
- [29] B. Ravindran et al., *Journal of Thermal Analysis and Calorimetry* **104**, 893 (2011)
- [30] H. Moradpoor et al., *Macedonian Journal of Medical Sciences* **7**(17), 2757 (2019).
- [31] N. L. L. Jeevigunta, R. V. Navva, *Research Journal of Biotechnology* **12**(10), (2017).
- [32] S. N. Rampersad, *Sensors* **12**(9), 12347 (2012).
- [33] F. Y. Ramírez-Castillo et al., *Pathogens* **4**, 307 (2015).
- [34] Q. Ma et al., *Antimicrobial Agents and Chemotherapy* **61**(6), e00308 (2017).
- [35] H. Liu et al., *Frontiers in Public Health* **6**, 159 (2018).
- [36] C. Ajonina et al., *Journal of Toxicology and Environmental Health* **78**, 381 (2015).
- [37] K. Kothhao et al., *Digest Journal of Nanomaterials and Biostructures*, **13**, 835 (2018).